Three Distinct F-Actin Binding Sites in the *Dictyostelium discoideum* 34 000 Dalton Actin Bundling Protein†

Rita W. L. Lim,‡ Ruth Furukawa,* Susan Eagle,§ Robert C. Cartwright,§ and Marcus Fechheimer

Department of Cellular Biology, University of Georgia, Athens, Georgia 30602

Received June 12, 1998; Revised Manuscript Received September 3, 1998

ABSTRACT: The *Dictyostelium* 34 kDa protein is an actin bundling protein composed of 295 amino acids. However, the region(s) of the molecule that bind actin filaments is (are) unknown. Studies of the cosedimentation of ^{125}I-34 kDa protein and F-actin show that the 34 kDa protein binds to F-actin with positive cooperativity and Hill coefficients of 1.9 and 3.0, for filaments 4.9 μm and 0.6 μm, respectively. The Hill coefficient is larger for short filaments that are more efficiently bundled than long filaments, suggesting that one of the binding sites is used in interfilament contacts or contributes to filament orientation within the bundle. Three distinct actin binding sites were identified using a synthetic peptide, protein truncations, and a novel epitope library screening method. The ability to bind actin was assessed by ^{125}I-F-actin overlays under denaturing and nondenaturing conditions, cosedimentation, viscometry, and pyrene-labeled actin disassembly. The three actin binding domains were identified as amino acids 1−123, 193−254, and 279−295. The 62 amino acid domain (193−254) can cosediment with F-actin. The estimated K_{app} obtained by the disassembly of pyrene-labeled actin was 0.11 μM and 2.7 μM for the amino acids 1−123 and 279−295, respectively. These results identify three distinct regions of the 34 kDa protein that may contribute to the positive cooperative formation of F-actin bundles.

Actin binding proteins contribute to the generation of cell shape and distinct morphological changes associated with essential physiological functions of cells. In the cellular slime mold *Dictyostelium*, these processes include chemotaxis, cytokinesis, locomotion, morphogenesis, and phagocytosis (*1*−*3*). Cells lacking various of these actin binding proteins created through gene replacement mediated by homologous recombination exhibit phenotypes which vary in type and severity (*4*−*8*). To date, 11 actin cross-linking proteins have been identified in *D. discoideum* (*9*), and the calcium-sensitive 34 kDa F-actin bundling protein is one of them. This protein constitutes just 0.04% of the total protein in the cell (*10*), yet it displays specific localization to filopodia and pseudopodia (*10*), early-forming phagocytic cups but not late phagocytic cups or late phagosomes (*11*, *12*), and cell-to-cell contact regions during development (*13*). Mutants lacking the 34 kDa protein have either longer filopodia or a higher density of short filopodia depending on the genotype of the parental strain. In addition, the mutant cells exhibit cytoplasmic shedding during crawling on a solid substratum and increased persistence in motility assays (*4*). Double mutation of the 34 kDa protein and other actin cross-linking proteins in *D. discoideum* results in more pronounced aberrant phenotypes (Rivero, F., Furukawa, R., Fechheimer, M., and Noegel, A. A., unpublished), suggesting some redundancy among the F-actin cross-linking proteins. Clearly, the 34 kDa protein is an important cytoskeletal component in *D. discoideum*.

In vitro biochemical analyses of the 34 kDa protein reveal that this monomeric protein does not interact with G-actin (*14*). Instead, the 34 kDa protein can cross-link and bundle actin filaments, and both activities are inhibited by calcium in the micromolar range (*10*, *15*). These data suggest the possibility of at least two F-actin binding regions within the polypeptide. Early structure and function experiments disclosed a division of actin binding activities within the 34 kDa protein. A 27 kDa core fragment generated from a limited α-chymotrypsin digestion could cross-link F-actin to form an isotropic network, but was unable to form anisotropic F-actin bundles. It lacked six amino acids from the N-terminus and an estimated 7 kDa fragment from the C-terminus of the 34 kDa polypeptide (*16*). Thus, in addition to two possible actin binding sites in the 27 kDa fragment, there may be other actin binding or bundle modulating activities in the regions missing from the 27 kDa fragment. Amino acid sequence analyses of the 34 kDa protein show weak homology to other actin-associated proteins, rabbit bisphosphate aldolase and *D. discoideum* gelation factor ABP 120 (*17*), although none of the similar regions resemble those of known actin binding sites. Comparison with other actin binding proteins in the database has failed to reveal any consensus actin binding sequences.

The present study seeks to identify actin binding sites in the 34 kDa protein. Using polymerase chain reaction (PCR)[1] cloning and heterologous recombinant protein expression technology, large quantities of the recombinant 34 kDa (r34 kDa) protein have been synthesized and purified from bacteria for biochemical studies (*18*). The recombinant form

† Supported by NSF Grant MCB 9808748.

* Corresponding author. E-mail: furukawa@cb.uga.edu. Fax: 706-542-4271.

‡ Present address: Department of Cell Biology, The Scripps Research Institute, La Jolla, CA.

§ Present address: Medical College of Georgia, Augusta, GA.

10.1021/bi981392d CCC: $18.00
Published on Web 12/16/1998

Table 1: Design of the Recombinant Truncated Forms of the 34 kDa Protein

protein	amino acids[a]	5′-primer[b]	3′-primer[b]
		Proteins Expressed in pET15b	
B9	1−240	GCAGAGGATCCGATGGCAGAAACAAAAGTTGC	CGATCTGGATCCTTAGGCAAAGTTGAGTTGTTC
C11	1−191	GCAGAGGATCCGATGGCAGAAACAAAAGTTGC	CGATAGGGATCCTTATTCGAGAGCTAAACGAGCTT
NT	1−123	GCAGAGGATCCGATGGCAGAAACAAAAGTTGC	GGATAGGGATCCTTATGGGTAGGTGGTTGCATAG
E3	77−295	GCAGAGGATCCGACAATCAAATATGCTGATATGC	ACGTAGGATTCCTTATTTCTTTTGTGGACCGT
CT	124−295	GCAGCTTCCATGGCTATCTCTCAACCACAAATGTTG	ACGTAGGATTCCTTATTTCTTTTGTGGACCGT
pG4	139−295	GCAGAGGATCCGTTAAGAGAAAAAGTCGATGTC	ACGTAGGATTCCTTATTTCTTTTGTGGACCGT
H1	71−240	GCAGAGGATCCGACAATCAAATATGCTGATATC	CGATCTGGATCCTTAGGCAAAGTTGAGTTGTTC
N12	124−240	GGCTGAGGATCCGATCTCTCAACCACAAATGTTG	CGATCTGGATCCTTAGGCAAAGTTGAGTTGTTC
O12	139−240	GCAGAGGATCCGTTAAGAGAAAAAGTCGATGTC	CGATCTGGATCCTTAGGCAAAGTTGAGTTGTTC
		Proteins Expressed as T7 Gene 10-Fusions in pET17xb	
	1−295	GCAGAGGATCCGATGGCAGAAACAAAAGTTGC	ACGTAGGATTCCTTATTTCTTTTGTGGACCGT
	1−123	GCAGAGGATCCGATGGCAGAAACAAAAGTTGC	GGATAGGGATCCTTATGGGTAGGTGGTTGCATAG
	1−53	GCAGAGGATCCGATGGCAGAAACAAAAGTTGC	CGACTGGATCCTTAATAAGCATTCAAAAAGTGAAC
	71−123	GCAGAGGATCCGACAATCAAATATGCTGATATC	GGATAGGGATCCTTATGGGTAGGTGGTTGCATAG
	124−240	GGCTGAGGATCCGATCTCTCAACCACAAATGTTG	CGATCTGGATCCTTAGGCAAAGTTGAGTTGTTC
	139−191	GCAGAGGATCCGTTAAGAGAAAAAGTCGATGTC	CGATAGGGATCCTTATTCGAGAGCTAAACGAGCTT
	139−240	GCAGAGGATCCGTTAAGAGAAAAAGTCGATGTC	CGATCTGGATCCTTAGGCAAAGTTGAGTTGTTC
		Protein Expressed as a GST-Fusion Protein in pGEX-2T	
G241	241−295	GAGCGTGGATCCCTTATCTCTGCTGAAGCTGC	ACGTAGGATCCTTATTTCTTTTGTGGACCGT

[a] Positions of the amino acid residues in the full-length, 295 amino acid, 34 kDa protein sequence (*18*). The CT (124−295) and E3 (77−295) which are expressed as nonfusion recombinant proteins. All other pET-15b constructs expressed histidine-fusion recombinant proteins. The 6X histidine leader is removed by thrombin cleavage, leaving 8 extra amino acids, GSHMLEDP, at the N-terminus of the protein. [b] Oligonucleotide primers used in PCR cloning, written in the 5′→3′ orientation. Restriction enzyme sites are *Bam*HI (single underline) and *Nco*I (double underline).

of the protein was characterized as functionally indistinguishable from the native protein isolated from *D. discoideum* (*18*). In this study, cosedimentation of ^{125}I-34 kDa protein with F-actin was utilized to characterize the affinity and cooperativity of the intact protein. In addition, the full-length and various truncated forms of the 34 kDa protein were synthesized in bacteria, purified, and assayed for their ability to interact with actin filaments. A combination of methods including ^{125}I-iodinated F-actin blot overlays, high-speed F-actin cosedimentation, low-shear falling-ball viscometry, and the disassembly of pyrene-labeled F-actin were used to disclose the locations of three distinct F-actin binding sites in the 34 kDa protein.

EXPERIMENTAL PROCEDURES

Materials. The *Pfu* DNA polymerase was purchased from Stratagene. The NovaTope system, His Bind resin, thrombin protease, the pET-15b, pET-17xb, and pET-32a vectors, and AD494(DE3) bacteria were purchased from Novagen. TALON beads were purchased from Clonetech. *N*-(1-Pyrenyl)iodoacetamide was purchased from Molecular Probes. Phalloidin was purchased from Boehringer Mannheim. Hydroxylapatite (HAP) came from Calbiochem. ^{125}I-Bolton−Hunter reagent was obtained from DuPont NEN. BCA protein assay reagent came from Pierce. Ovalbumin 2× crystallized came from Worthington. Nitrocellulose membranes (0.45 μm, BA-85) were purchased from Schleicher & Schuell. Alkaline phosphatase conjugated goat anti-rabbit and anti-mouse antibodies were purchased from Promega. Fmoc-amino acids and resins were purchased from Advanced ChemTech.

Synthetic Peptide. The synthetic peptide was made with an Advanced ChemTech Model MPS 350 automated peptide synthesizer (Louisville, KY) using Fmoc chemistry according to the manufacturer's protocol at the University of Georgia Molecular Genetics Instrumentation Facility. The 17 amino acid peptide (norleucine-NRDLEEKKKRYGPQKK) corresponds to the amino acid sequence Met^{279}−Lys^{295} at the C-terminus of the 34 kDa protein. The more stable norleucine amino acid was used to replace Met^{279} in the synthetic peptide.

Design of Expression Vectors. All molecular methods were performed according to Sambrook et al. (*19*). Construction of the recombinant full-length 34 kDa protein (r34 kDa) expression vector, pET-15b-F18, has been described (*18*). Other truncated forms of the 34 kDa protein were made by PCR cloning of the *D. discoideum* 34 kDa protein cDNA template in pBSK30 (*17*, *18*) according to the conditions previously described for the r34 kDa protein (*18*). Table 1 summarizes the truncated proteins made, the specific regions of the 34 kDa protein present in the truncated proteins, their respective expression vectors, and their PCR cloning primers. These primers were designed to amplify specific regions of the 34 kDa protein cDNA using the *Pfu* DNA polymerase and to facilitate the ligation of the amplified DNA into the expression vectors. Each primer has 1 restriction enzyme recognition site (*Bam*HI or *Nco*I) and at least 20 nucleotides overlapping with the cDNA template. DNA amplifications were conducted in a Perkin-Elmer Cetus Model 480 DNA thermal cycler (Perkin-Elmer, Norwalk, CT). The amplified DNA segments were digested with the appropriate restriction enzymes and ligated into the expression vectors. The pET-plasmid constructs and pGEX-2T constructs were transformed into the expression host bacteria BL21(DE3) and

[1] Abbreviations: r34 kDa, recombinant 34 kDa protein; CB, carbenicillin; tet, tetracycline; MES, 2-(*N*-morpholino)ethanesulfonic acid; HAP, hydroxylapatite; CM, carboxymethyl; DEAE, diethylaminoethyl; Fmoc, *N*-(9-fluorenyl)methoxycarbonyl; BCA, bicinchoninic acid; PMSF, phenylmethylsulfonyl fluoride; PBS, phosphate-buffered saline; SDS, sodium dodecyl sulfate; DTT, dithiothreitol; β-ME, β-mercaptoethanol; PIPES, piperazine-*N*,*N*′-bis(2-ethanesulfonic acid); GST, glutathione-*S*-transferase; TRX, thioredoxin; IPTG, isopropyl-1-thio-galactopyranoside; PCR, polymerase chain reaction; bp, base pair(s).

BL21, respectively. The fragment T193 (193−254) was derived by excising the fragment corresponding to amino acids 193−254 in the TvecCB/tet clone (based on the pTOPE vector, see below) with *Bam*HI and *Xho*I and ligating into the pET-32a vector previously digested with *Bgl*II and *Xho*I. The pET-32a construct was transformed into the expression host bacteria AD494(DE3). The open reading frames in these constructs were verified by automated DNA sequencing conducted at the University of Georgia Molecular Genetics Instrumentation Facility with a Perkin-Elmer Applied Biosystems Instrument 373 using the *Taq* DNA polymerase, fluorescence detection, and dideoxy terminator chemistry (*20*). The pET-15b E3 (77−295) construct was detected to have a frame shift within the 34 kDa protein coding region due to a duplication of 11 nucleotides at the 5′ end of the amplified 34 kDa protein DNA segment. Premature termination of protein translation was predicted to occur after the third codon in the specified 34 kDa protein sequence. However, translation was reinitiated at a nearby ATG codon 9 nucleotides downstream of the misplaced stop codon. This ATG start codon corresponds to Met^{77} in the 34 kDa protein sequence. Bacterial host cells carrying the pET-15b E3 (77−295) construct expressed an ∼25 kDa protein only upon induction with IPTG. Western blot analyses using polyclonal rabbit anti-34 kDa protein antibodies (*10*) and a monoclonal mouse B2C antibody (*11*) that recognizes only the C-terminal two-thirds of the 34 kDa protein (Lim and Fechheimer, unpublished) were conducted to confirm that this recombinant 25 kDa protein indeed contained amino acid sequences of the 34 kDa protein (data not shown).

Expression and Purification of Recombinant Proteins. Growth of the expression bacteria, induction of protein expression with IPTG, harvest, and storage of bacteria were conducted as reported for the r34 kDa protein (*18*), except that the expression of all histidine-fusion proteins was induced with 0.5 mM IPTG instead of 1 mM. The full-length r34 kDa protein was expressed and purified as previously described (*18*). All purification steps were performed at 4 °C.

The histidine-fusion proteins were purified by nickel metal affinity chromatography. The pET-15b-based constructs were designed to express N-terminal cleavable histidine-fusion proteins except for CT (124−295) and E3 (77−295), which were expressed as nonfusion proteins. Bacteria harvested from 100 mL of culture were resuspended in 20 mL of cold lysis buffer (50 mM Tris-HCl, pH 8.0, 2 mM EDTA, 10% glycerol, 1% Triton X-100, 1 mM PMSF, and 0.2 mg/mL lysozyme) and stirred for 1 h to allow complete cell lysis. The lysate was placed in an ice/ethanol bath and sonicated (6 × 30 s) at 30% output for the microtip (Branson-Sonifier cell disruptor 200) to shear the DNA. The lysate was centrifuged at 25000*g* for 15 min, and the supernatant was discarded. The pellet, which contained >95% of the expressed recombinant protein as insoluble inclusion bodies, was resuspended in 20 mL of PBS, pH 7.4, 25% sucrose, 1% Triton X-100, and 5 mM EDTA (buffer A). A brief 15 s sonication pulse was given to aid in resuspension. The mixture was centrifuged as stated above, and the pellet was washed 2 more times with buffer A. The pellets were washed a fourth time with cold deionized water to remove EDTA prior to solubilization in denaturant and subsequent histidine affinity purification under denaturing conditions. The histidine-fusion proteins were affinity-purified on the His Bind resin under denaturing conditions with a few modifications to the manufacturer's protocol. The pellet of inclusion bodies was solubilized in 25 mL of denaturation buffer (6 M urea, 20 mM Tris-HCl, pH 8.0, 5 mM imidazole hydrochloride, pH 8.0, and 0.5 M NaCl) for 1 h with periodic Dounce homogenization. This denaturation buffer was freshly prepared with Amberlite MB-3A mixed ion exchange purified urea. The solution of denatured proteins was clarified at 39000*g* for 45 min, and the supernatant was applied onto a 2.5 mL His Bind column. Prior to use, the resin in the column was rinsed with 7.5 mL of cold deionized water, cation-charged with 12.5 mL of 50 mM Ni^{2+}, and equilibrated with 7.5 mL of the denaturation buffer according to the manufacturer's procedure. After the complete application of the supernatant, the column was washed with 25 mL of denaturation buffer followed by 15 mL of denaturation buffer containing 20 mM imidazole. The histidine-fusion protein was step-eluted with the denaturation buffer containing 1 M imidazole. The fractions with the protein of interest were identified by SDS−PAGE. These fractions were pooled (∼5 mL) and gradually diluted to 1 M urea and 0.2 mg/mL protein concentration with 50 mM Tris-HCl, pH 9.0, 20% glycerol, 0.25 M NaCl, 1 mM EDTA, and 1% NP-40 over a period of 1 h. The urea was removed by sequential dialysis against 4 L of 50 mM Tris-HCl, pH 9.0, 0.25 M NaCl, 10% glycerol, and 1 mM EDTA, followed by three changes with 4 L of 20 mM Tris-HCl, pH 8, and 0.15 M NaCl over a 36 h period. The renatured histidine-fusion proteins were purified on the His Bind column under nondenaturing conditions according to the manufacturer's protocol. Na-EDTA, pH 8.0, was added to the eluted protein to a final concentration of 0.1 mM, and the protein was dialyzed against 4 L of 20 mM Tris-HCl, pH 8.0, 0.1 M NaCl, and 0.02% NaN_3 (buffer B) followed by 4 L of buffer B with 0.1 mM DTT. The proteins obtained were ≥90% pure with an average yield of 2.5 mg of protein/100 mL of bacteria culture. After the nickel affinity purification, the histidine leader peptide was removed by thrombin cleavage, leaving eight extra amino acid residues (GSHMLEDP) at the N-terminus of the protein. The cleavage mixture contained 0.5 IU/mL thrombin and 0.5 mg/mL protein in 20 mM Tris-HCl, pH 8.4, 0.15 M NaCl, and 2.5 mM $CaCl_2$. The mixture was agitated gently at 20 °C for 16 h, and the reaction was terminated with the addition of PMSF and Na-EDTA, pH 8.0, to final concentrations of 1 mM and 0.5 mM, respectively. The salts in the cleavage mixture were removed by dialysis against 10 mM Tris-HCl, pH 8.0, 0.1 mM PMSF, 0.1 mM EDTA, and 1 mM β-ME, and then followed by 10 mM MES−NaOH, pH 6.5, 0.1 mM PMSF, 0.1 mM EDTA, and 5 mM β-ME (buffer C). The dialyzed solution was applied onto a 0.6 × 3.0 cm CM-52 column equilibrated with buffer C. The protein was eluted with 200 mL of 0−0.2 M NaCl linear gradient in buffer C. The eluted protein was pooled, dialyzed against storage buffer (20 mM Tris-HCl, pH 8.0, 0.1 M KCl, 0.2 mM DTT, and 0.02% NaN_3), divided into small aliquots, and stored at −80 °C.

The inclusion body pellets of the nonfusion recombinant proteins, CT (124−295) and E3 (77−295), were prepared from the bacterial host as described above. Depending on the size, the pellet obtained from 1 L of bacterial culture was solubilized in 25−80 mL of 50 mM Tris-HCl, pH 9.0,

5 mM EDTA, 6 M urea or guanidine hydrochloride, 1 mM PMSF, and 5 mM β-ME for 1 h with periodic Dounce homogenization. After centrifugation at 39000*g* for 1 h, the supernatant was collected and gradually diluted to 1 M urea or guanidine hydrochloride and 0.2 mg/mL protein concentration with 50 mM Tris-HCl, pH 9.0, 20% glycerol, 0.15 M NaCl, 1 mM EDTA, and 15 mM β-ME over 1 h. The denaturant was removed by sequential dialysis against 20 volumes of each of the following buffers: 50 mM Tris-HCl, pH 8.0, 0.25 M NaCl, 1 mM EDTA, and 15 mM β-ME; 20 mM Tris-HCl, pH 8.0, 50 mM NaCl, 1 mM EDTA, and 1 mM β-ME; and 10 mM Tris-HCl, pH 8.0, 0.1 mM EDTA, and 1 mM β-ME over a period of 36 h. The renatured protein was applied onto a 2 × 15 cm DE-52 column equilibrated with 10 mM Tris-HCl, pH 8, 0.1 mM EDTA, and 1 mM β-ME. The fraction not bound to the DE-52 column which contained most of the recombinant proteins was collected, and the pH was adjusted to 6.5 with 1 M MES. For the E3 (77−295) protein, the DE-52 unbound fraction was applied onto a 1 × 10 cm CM-52 column equilibrated with 10 mM Tris−MES, pH 6.5, 0.1 mM EDTA, and 1 mM β-ME (buffer D), and eluted with a 500 mL 0−0.3 M NaCl gradient in buffer D. E3 (77−295) was eluted at 75 mM NaCl. For the CT (124−295) protein, the DE-52 unbound fraction was applied onto a 1 × 10 cm HAP column equilibrated with buffer D, and eluted with 200 mL of a 0−0.2 M phosphate gradient in buffer D. CT (124−295) was eluted at 0.12 M phosphate. Eluted proteins were dialyzed against buffer D prior to concentration. In both cases, the proteins were concentrated on 0.5 × 2.5 cm HAP columns by step elution with 0.2 M phosphate in buffer D, dialyzed against storage buffer, and stored as described above. The average yield of ∼90% purity was 3 mg of protein/L and 25 mg of protein/L of bacterial culture for CT (124−295) and E3 (77−295), respectively.

The proteins expressed from pET-17xb-based constructs were N-terminal T7 gene 10-fusion proteins. The 260 amino acid T7 gene 10 leader peptide could not be cleaved, and experiments were conducted with the fusion proteins. The inclusion body pellets of T7 gene 10-fusion proteins were collected as described above, solubilized directly in SDS−PAGE sample buffer, and used without further purification.

The pGEX-2T-based construct expressed the N-terminal GST-fusion protein, G241 (241−295). No attempt was made to remove the 27 kDa GST leader. The pellet from a 100 mL bacterial culture was resuspended in 10 mL of cold lysis buffer (PBS, pH 7.4, 1 mM EDTA, 1% Triton X-100, 0.1% NP-40, 1 mM PMSF, 1 mM benzamidine, 1 mM benzamide, 5 mM caproic acid, 0.5 mg/mL leupeptin, and 0.2 mg/mL lysozyme) and stirred 30 min. The lysate was placed in an ice/ethanol bath, and the DNA was sheared by sonication (2 × 30 s). The lysate was centrifuged at 10000*g* for 15 min. The supernatant was mixed with 1 mL of glutathione agarose equilibrated with PBS, pH 7.4. The suspension was gently agitated for 30 min and then centrifuged at 500*g* for 5 min. The supernatant was discarded, and the glutathione agarose was washed 3 times with 10 mL of cold PBS, pH 7.4. The G241 (241−295) was eluted from the agarose with 1 mL of 10 mM reduced glutathione in 50 mM Tris-HCl, pH 8.0. NaN_3 and KCl were added to the final concentrations of 0.02% and 100 mM, respectively. The G241 (241−295) was divided into small aliquots and stored at −80 °C. Average yield was 2.5 mg of protein/100 mL of bacterial culture with a purity of ∼90%.

The pET-32a-based construct expressed the N-terminal fusion protein histidine-tagged thioredoxin T193 (193−254). No attempt was made to remove the thioredoxin leader. The pellet from a 500 mL bacterial culture was resuspended in 30 mL of cold lysis buffer (20 mM Tris, pH 7.9, 100 mM NaCl, 1 mM PMSF, 1 mM benzamidine, 1 mM benzamide, 5 mM caproic acid, 0.5 mg/mL leupeptin, and 0.75 mg/mL lysozyme) and stirred 1 h. The lysate was placed at −20 °C for 1 h and subsequently into an ice/ethanol bath, and the DNA was sheared by sonication (2 × 30 s). The lysate was centrifuged at 150000*g* for 30 min. The supernatant was diluted 3-fold with 20 mM Tris, pH 8.0, 500 mM NaCl (buffer E) and applied to a column with 0.75 mL of talon beads equilibrated with buffer E supplemented with 5 mM imidazole. The column was washed with 20 mL of buffer E with 5 mM imidazole, followed by 10 mL of buffer E with 10 mM imidazole, and eluted with a linear 50 mL gradient from 10 mM to 333 mM imidazole. The T193 (193−254) was dialyzed versus 20 mM Tris, pH 8.0, 100 mM KCl, 0.02% NaN_3, and 5 mM β-mercaptoethanol, divided into small aliquots, and stored at −80 °C. Similar preparative methods were used to purify the thioredoxin leader from the pET-32a vector with no insert for use as a control.

Construction of the Epitope Expression Library. The NovaTope system was used to construct the epitope library that expressed short protein sequences derived from the C-terminal 171 amino acids of the 34 kDa protein, the CT (124−295) protein. The target DNA was generated from the pET-15b CT (124−295) construct by two different methods: (1) restriction enzyme digestion with *Nco*I and *Bam*HI to liberate the DNA segment of ∼520 bp; and (2) three sequential rounds of PCR amplification of the same coding region. Following the manufacturer's recommendations, this segment of DNA was digested with DNase I in the presence of Mn^{2+} to give small DNA fragments of various sizes. The DNA fragments of 50−150 and 150−300 bp ranges were isolated by gel electrophoresis followed by electroelution. The fragments were blunt-ended by T4 DNA polymerase, 3′-dA-tailed by *Tth* DNA polymerase, and ligated into linearized pTOPE T-vectors (Tvec). The T-vectors were transformed into NovaBlue(DE3) expression bacteria, plated on LB agar supplemented with 50 μg/mL carbenicillin (CB) and 15 μg/mL tetracycline (tet), and grown overnight at 37 °C. The small DNA fragments were expressed as N-terminal T7 gene 10-fusion proteins. These TvecCB/tet clones were replica-plated onto nitrocellulose membranes and screened for F-actin binding by the ^{125}I-F-actin overlay assay. Positive clones were rescreened, and the size of the DNA fragment in each clone was estimated by bacterial colony PCR using the T7 gene 10 primer and T7 terminator primer supplied by Novagen. The sequences of the 34 kDa protein DNA fragments found in the TvecCB/tet clones were obtained by automated DNA sequencing as described above. In addition to these positive clones, several clones expressing in-frame fragments of 34 kDa protein that did not bind F-actin were also sequenced.

Actin. Sephadex-G150 column purified G-actin was prepared from rabbit skeletal muscle acetone powder (*21*, *22*) and maintained in G-actin buffer (2 mM Tris-HCl, pH 8.0, 0.2 mM $CaCl_2$, 0.2 mM ATP, 0.2 mM DTT, and 0.02%

NaN_3) at 4 °C for up to 1 week with daily buffer changes. After 1 week, the G-actin was subjected to a cycle of polymerization under high-salt conditions (50 mM KCl, 1 mM ATP, 1 mM $MgCl_2$) and then depolymerization by dialysis against G-actin buffer before maintenance in G-actin buffer.

G-Actin (4−5 mg/mL) was iodinated with ^{125}I-monoiodinated Bolton−Hunter reagent at free amino groups of the actin molecule as described (*23*, *24*), and the average specific activity was ∼54 μCi/mg of protein. Gelsolin-capped phalloidin-stabilized ^{125}I-F-actin was made as described previously (*25*) by the polymerization of ^{125}I-G-actin in the presence of 20 mM PIPES, pH 7.0, 50 mM KCl, 2 mM $MgCl_2$, 1 mM ATP, 0.5 mM $CaCl_2$, and 1:100 molar ratio of gelsolin to actin for 30 min at room temperature, followed by filament stabilization with a 1.5 molar excess of phalloidin. Gelsolin was purified from pig serum by a modification of Cooper et al. (*26*) as previously described (*27*). Prior to use in the ^{125}I-F-actin overlay assays, the F-actin was diluted to an actin concentration of 0.5 mg/mL with TBST (10 mM Tris-HCl, pH 7.5, 90 mM NaCl, and 0.5% v/v Tween-20) containing 5% (w/v) nonfat dry milk, 5 μM phalloidin, and 0.02% NaN_3 (*25*). This diluted sample was stored at 4 °C.

F-Actin was labeled with *N*-(1-pyrenyl)iodoacetamide in 100 mM H_3BO_3, pH 8.5, 100 mM KCl, and 0.4 mM $MgCl_2$ under nitrogen for 3−5 h at room temperature. The mixture was dialyzed overnight against 2 mM PIPES, pH 7.0, 100 mM KCl, 2.0 mM $MgCl_2$, 0.5 mM ATP, 0.5 mM DTT, and 0.02% NaN_3. The F-actin was collected by centrifugation at 165000*g* for 2 h at 4 °C, depolymerized by dialysis in G-actin buffer, and purified on Sephadex G-150. The average preparation had ∼90% of the actin labeled with pyrene. The pyrene-labeled G-actin was maintained as described for the unlabeled G-actin except the pyrene-labeled G-actin was shielded from light to prevent photobleaching.

Production of the Dictyostelium 34 kDa Protein. The 34 kDa protein was purified from *D. discoideum* as previously described (*28*). The 34 kDa protein was iodinated with ^{125}I-monoiodinated Bolton−Hunter reagent at free amino groups of the molecule as described (*13*), and the average specific activity was ∼180 μCi/mg of protein.

Production of the 27 kDa Protein Fragment. The 27 kDa protein was purified from a limited α-chymotrypsin digestion of the *D. discoideum* 34 kDa protein using HAP column chromatography as previously described (*16*).

Actin Interaction Assays. F-Actin high-speed cosedimentation assays were performed as described previously (*10*, *15*, *18*). The solutions were centrifuged in a Beckman airfuge at 23 psi (115000*g*) for 30 min. The supernatant (S) and the pellet (P) samples were collected and analyzed by SDS−PAGE and Coomassie Blue staining.

The binding of the ^{125}I-34 kDa protein to actin was investigated in two ways. Solutions contained either a fixed concentration of actin and varying amounts of ^{125}I-34 kDa protein (4.6×10^3 cpm/μg of protein) or a fixed concentration of ^{125}I-34 kDa protein (1×10^5 cpm/μg of protein) and varying concentrations of actin. Solutions containing either ^{125}I-34 kDa protein (0.02−6 μM) and G-actin (24 μM): gelsolin at a ratio of 222:1 or 1778:1 or ^{125}I-34 kDa protein (0.25 μM) and G-actin (2.4−24 μM):gelsolin at a ratio of 222:1 or 1778:1 were polymerized in 20 mM PIPES, pH 7.0, 50 mM KCl, 50 μM $MgCl_2$, 0.2 mM DTT, 2.5 mM EGTA, 0.02% NaN_3, and 1 mg/mL ovalbumin for 2 h at room temperature. The solutions were centrifuged as described above in centrifuge tubes that were previously coated with 1 mg/mL ovalbumin and allowed to air-dry. The supernatant sample was collected, and the pellet was washed twice briefly with ice-cold 20 mM PIPES, pH 7.0, 50 mM KCl, 50 μM $MgCl_2$, 0.2 mM DTT, 2.5 mM EGTA, 0.02% NaN_3, and 1 mg/mL ovalbumin before the radioactivity in the samples was measured in a gamma counter (Beckman 4000). The total radioactivity in the pellet sample was corrected for the amount of ^{125}I-34 kDa protein that either bound to the centrifuge tube or sedimented without actin. The data were analyzed using the Hill plot (*29*).

The low-shear falling-ball viscometry assay was performed as previously described (*16*, *18*, *30*) using 4.7 μM F-actin and 0.05−0.5 μM samples of the truncated forms of the 34 kDa protein. The recombinant truncated proteins were scored for their ability to significantly increase the viscosity of the F-actin solution over that of F-actin alone (≥4×) at the concentration range that has been previously determined for the full-length 34 kDa protein (*16*, *18*).

The F-actin disassembly assay using pyrene-labeled actin was performed as described previously (*14*). Pyrene-labeled G-actin (2 μM) was polymerized overnight in assay buffer (25 mM Tris-HCl, pH 7.4, 0.14 M KCl, 2 mM $MgCl_2$, 1 mM EGTA, 0.2% NP-40, and 1 mM ATP). F-Actin disassembly was initiated by diluting the actin solution 20-fold with assay buffer containing increasing amounts of the α-chymotryptic digest 27 kDa fragment, the NT (1−123) protein, or the 2 kDa synthetic peptide (279−295). The decrease in pyrene fluorescence intensity (370 nm excitation, 410 nm emission) was monitored with a Perkin-Elmer LS-5 fluorescence spectrophotometer for 60 min. The initial rates of decrease in intensity were calculated and used in the estimation of apparent dissociation constants.

The ^{125}I-F-actin overlay blot assays were adapted from Chia et al. (*25*). For bacterial colony blots, individual colonies of bacteria were grown directly on nitrocellulose membranes overnight at 37 °C. The bacteria were induced to express protein with 1 mM IPTG for 3 h. This induction step was omitted for the TvecCB/tet bacteria generated by the NovaTope system. The colonies on the membrane were lysed and permeabilized in a chloroform chamber for 15 min and subsequently incubated in freshly prepared 20 mM Tris-HCl, pH 8.0, 6 M urea, and 0.5 M NaCl for 15 min. The membrane was blocked in TBST with 5% (w/v) nonfat dry milk for 1 h and washed twice with TBST for 15 min each to remove excess cell debris. The membrane was overlaid with ^{125}I-F-actin solution with gentle shaking for 2 h at room temperature. The membrane was subsequently washed in TBST (8 mL/100 mm filter circles) for 1 min, air-dried, and exposed to Kodak X-OMAT film with an intensifying screen at room temperature for a period of 3−4 days (for primary screens) or 1 day (for secondary screens). For SDS−PAGE denatured protein blots, the proteins (150 pmol) were separated on 15% SDS−PAGE gels and electrophoretically transferred onto nitrocellulose membranes at 66 V for 3 h at 4 °C. For SDS-treated protein dot blots, the proteins (150 pmol) were treated with SDS−PAGE sample buffer, diluted 50-fold with 50 mM Tris-HCl, pH 8.0, and dot-blotted onto nitrocellulose membranes. For non-SDS-treated protein blots,

the proteins (50 and 150 pmol) were directly dot-blotted onto nitrocellulose membranes. All protein blots were processed in the same manner as the bacterial colony blots except that the TBST washes prior to the application of ^{125}I-F-actin were omitted.

Protein Analytical Methods. Protein concentrations were determined by the BCA method (*31*) using bovine serum albumin as the protein standard. Protein samples were analyzed on 15% SDS−PAGE according to Laemmli (*32*) and visualized by Coomassie Brilliant blue staining. Western blot analyses were performed as described by Towbin (*33*), using rabbit polyclonal anti-34 kDa antibodies (*10*), monoclonal B2C mouse anti-34 kDa antibody (*11*), and alkaline phosphatase conjugated goat anti-rabbit and anti-mouse antibodies.

RESULTS

Cooperative Binding of the 34 kDa Protein to F-Actin. The binding of ^{125}I-34 kDa protein to F-actin was studied at two filament lengths, since the order of filaments within bundles formed with the 34 kDa protein was found to be length-dependent (*34*). The cosedimentation assay was utilized, and the data were analyzed using the Hill plot (Figure 1). The nature of the binding of the 34 kDa protein to F-actin is length-dependent (Figure 1A). The binding of the 34 kDa protein to F-actin saturated at a stoichiometry of 1:18. The slope of the Hill plot was determined to be 3.0 or 1.9 for filaments 0.6 μm and 4.9 μm, respectively, using values of log [34 kDa protein] free between 0.1 and 0.9 (Figure 1B,C). These values suggest that the minimum number of apparent actin binding sites is 3 and that the number of binding sites observed is length-dependent. The value of K′ was calculated to be 1.2 μM independent of filament length.

Generation of Recombinant Truncated Proteins. To localize the actin binding sites in the *D. discoideum* 34 kDa protein, our experimental approach was to synthesize specific regions of the 34 kDa protein as recombinant proteins and probe their actin binding activities by several different F-actin binding assays. In a previous report, the recombinant 34 kDa (r34 kDa) protein was successfully cloned by PCR, expressed, and purified from bacteria. In vitro, the r34 kDa protein bound F-actin in a Ca^{2+}-dependent manner and was functionally indistinguishable from the native 34 kDa protein from *D. discoideum* (*18*). This set the precedent for the syntheses of truncated 34 kDa proteins using similar molecular techniques. In all, 18 different expression constructs were made (Table 1), representing 14 truncated forms of the 34 kDa protein (Figure 2). Smaller regions of the 34 kDa protein, 1−53, 71−123, 139−191, 193−254, and 241−295, were expressed as T7 gene 10-fusion, TRX-fusion, or GST-fusion proteins to aid in protein expression.

All the truncated forms of the 34 kDa protein were expressed at high levels in the host bacteria, ranging from 10 to 25% of the total cell protein. Unlike the r34 kDa protein, most of the truncated proteins were found exclusively in the insoluble fraction of the host cell, and hence were purified from the insoluble fractions. The CT (124−295) was, however, found to be evenly distributed in the soluble and insoluble fractions, but purification of the CT (124−295) was attempted only from the insoluble fraction due to ease

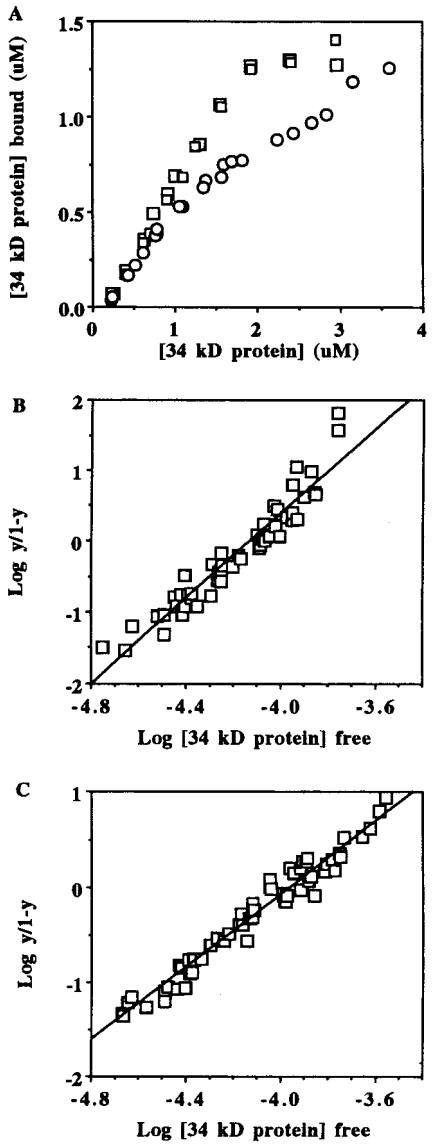

FIGURE 1: Hill plot of the binding of ^{125}I-34 kDa protein to F-actin. The concentration of 34 kDa protein bound to F-actin as a function of the total concentration of 34 kDa protein (A). The actin filaments were 0.6 μm (□) and 4.9 μm (○). Measurements were performed in duplicate. Similar results were obtained in independent experiments. log (y/1 − y) versus log [free 34 kDa protein] is plotted where y is the fraction of total sites occupied. The slope between log (y/1 − y) values of 0.1 and 0.9 was determined for two different filament lengths, 0.6 μm (B) and 4.9 μm (C), with five independent trials. The apparent Hill coefficients are 3.0 and 1.9 for the 0.6 μm and 4.9 μm filaments, respectively. The value of K′ is 1.2 μM independent of filament length.

of the inclusion body purification procedure. The purification yields of the various fragments ranged from 3 to 25 mg of protein of ~90% purity per liter of bacterial culture. The majority of the expressed G241 (241−295) and T193 (193−254) were found in the soluble fraction of the bacterial lysates, and were purified from the soluble fraction using glutathione agarose and talon bead affinity chromatography, respectively.

Mapping F-Actin Binding with ^{125}I-Labeled F-Actin. The SDS-denatured native 34 kDa protein and the 27 kDa α-chymotryptic digest fragment were reported to bind ^{125}I-F-actin on blots (*16*, *25*, *35*). To broadly localize the ^{125}I-F-actin binding region(s) to the amino- and/or carboxyl-

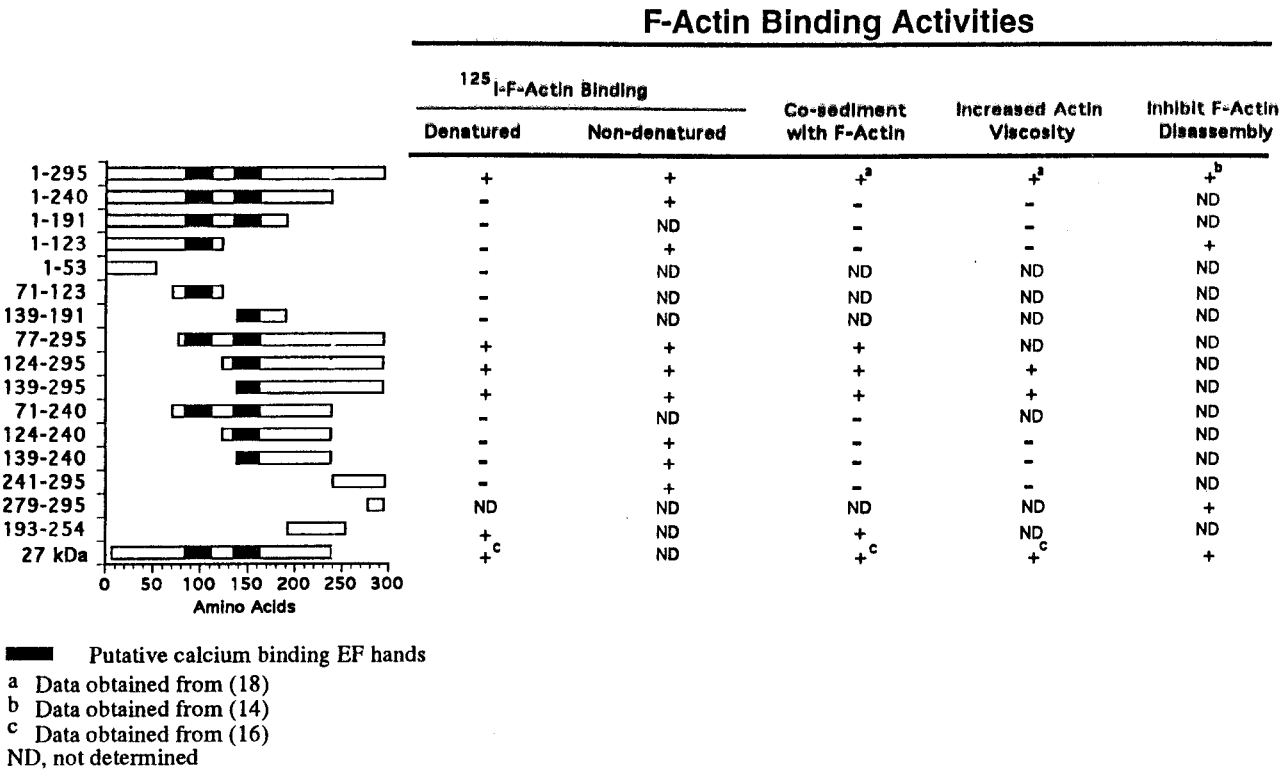

FIGURE 2: Summary of the F-actin binding activities of the full-length and truncated forms of the 34 kDa protein. The various truncated forms are denoted by the amino acid residue positions (shown on the left) corresponding to the specific regions in the full length 295 amino acid protein. The shaded boxes are putative calcium binding EF-hand motifs. All proteins were bacterially expressed recombinant proteins except for the 2 kDa synthetic peptide 279−295 and the 27 kDa α-chymotryptic digest fragment (*16*). The interactions of the truncated proteins with actin filaments were determined by ^{125}I-F-actin blot overlays (*25*, *35*) under native or SDS/urea denatured conditions, high-speed cosedimentation assays (*15*), viscometry (*30*), and the disassembly of pyrene-labeled F-actin (*14*).

terminal portion of the 34 kDa protein, the two major nonoverlapping regions of the 34 kDa protein, NT (1−123) and CT (124−295), were analyzed. The bacteria expressing either the NT (1−123), the CT (124−295), the r34 kDa protein, or only the histidine leader peptide encoded by the pET-15b plasmid were grown directly on nitrocellulose membranes, induced with IPTG to synthesize the encoded protein, and lysed in chloroform. The proteins were denatured in urea and subsequently assayed for F-actin binding activity. Both the r34 kDa protein and the CT (124−295) bound ^{125}I-F-actin, while the NT (1−123), the histidine leader peptide, and bacterial proteins from BL21(DE3) pET-15b (no DNA insert) did not (Figure 3).

To search for other F-actin binding domains within the 34 kDa protein that could have been missed in the initial NT (1−123)/CT (124−295) experiment, a collection of recombinant proteins was produced and analyzed. The proteins r34 kDa, B9 (1−240), C11 (1−191), NT (1−123), E3 (77−295), CT (124−295), pG4 (139−295), H1 (71−240), N12 (124−240), O13 (139−240), and G241 (241−295) and the T7 gene 10-fusion proteins (1−295), (1−123), (1−53), (71−123), (139−191), (124−240), and (139−240) were separated by SDS−PAGE, electrophoretically transferred onto nitrocellulose membranes, and screened for ^{125}I-F-actin binding (Figure 4A). Only the r34 kDa protein, E3 (77−295), CT (124−295), pG4 (139−295), and the T7 gene 10-fusion (1−295) bound ^{125}I-F-actin, with the minimum common sequence among them being 139−295. The extra eight amino acids (GSHMLEDP) found at the N-terminus of all the cleaved histidine-fusion proteins did not affect

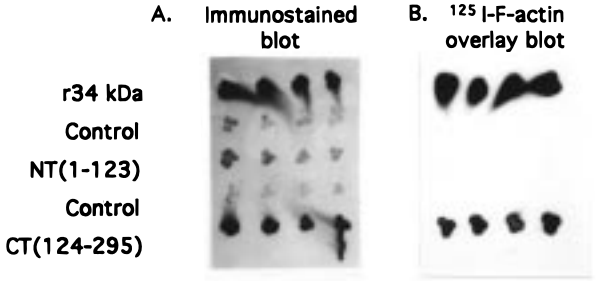

FIGURE 3: Recombinant full-length 34 kDa protein and the CT (124−295) protein bound ^{125}I-F-actin on bacterial colony blots. Bacteria expressing the full-length 34 kDa protein, the NT(1−123), the CT(124−295), and the histidine leader peptide [control bacteria BL21(DE3) pET-15b (no insert)] were grown on nitrocellulose membranes. Following protein expression and cell lysis, the membranes were blocked, washed, and then probed with either rabbit polyclonal anti-34 kDa protein antibodies followed by alkaline phosphatase-conjugated goat anti-rabbit antibodies (A) or gelsolin-capped phalloidin-stabilized ^{125}I-F-actin followed by autoradiography (B).

F-actin binding since pG4 (139−295) bound ^{125}I-F-actin as well as the nonfusion proteins CT (124−295) and E3 (77−295) (Figure 4A). The 260 amino acid residue T7 gene 10 leader protein did not bind F-actin nor did it affect the actin binding activity of the T7 gene 10-fusion (1−295) protein (Figure 4B). Similarly, the 27 kDa GST leader protein (Figure 4A) did not bind F-actin.

Since the ^{125}I-F-actin blot overlay assays involved studying the proteins after denaturation with SDS and treatment with reducing agent, any F-actin binding activity resulting from

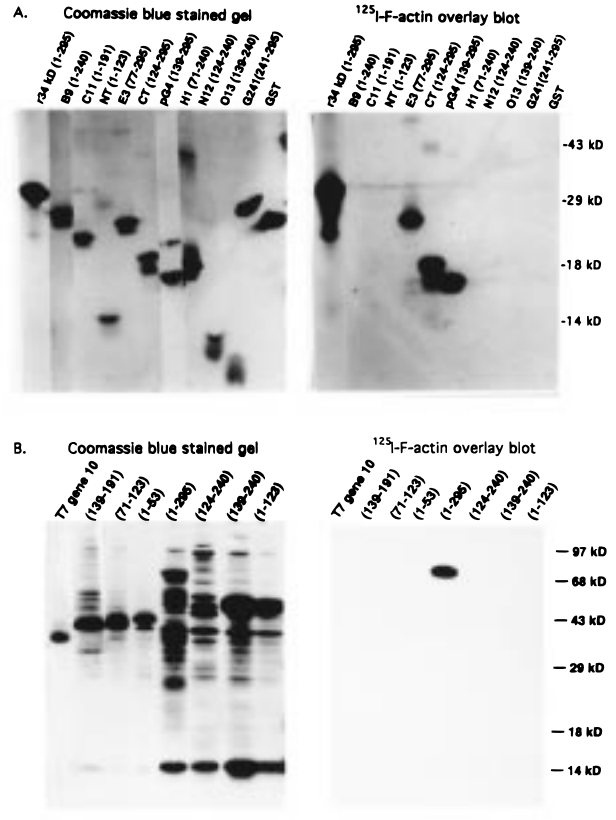

FIGURE 4: Binding of the full-length and truncated 34 kDa proteins to ^{125}I-F-actin on blots under denaturing conditions. Coomassie Blue stained 15% SDS−PAGE gels and autoradiograms of ^{125}I-F-actin overlays of nitrocellulose membrane blots obtained by electrophoretic transfer of proteins from SDS−PAGE gels. (A) Purified recombinant proteins (150 pmol each) derived from the pET-15b and pGEX-2T expression vectors. (B) T7 gene 10-fusion proteins (150 pmol) derived from the pET-17xb expression vector were partially purified as inclusion bodies and solubilized in SDS sample buffer prior to SDS−PAGE.

conformationally sensitive regions of the 34 kDa polypeptide could have been overlooked. To uncover such regions, native non-SDS-treated proteins were analyzed in ^{125}I-F-actin dot blot overlays. Both SDS- and non-SDS-treated E3 (77−295), CT (124−295), pG4 (139−295), and the r34 kDa protein interacted with ^{125}I-F-actin (Figure 5), consistent with the results obtained for the ^{125}I-F-actin blots of SDS−PAGE resolved and electrophoretically transferred proteins (Figure 4). The actin binding activities were distinctly detected when only 50 pmol of these four proteins was used under non-SDS denaturing conditions. On the other hand, ^{125}I-F-actin binding was detected with 150 pmol, but not with 50 pmol of the B9 (1−240), NT (1−123), N12 (124−240), O13 (139−240), and G241 (241−295) proteins (Figure 5A). These apparently weaker actin binding activities were eliminated upon SDS treatment (Figure 5B). Nonspecific binding of ^{125}I-F-actin to non-34 kDa derived proteins such as the GST-fusion leader was not observed.

The common region of 139−295 in the 34 kDa protein was able to bind ^{125}I-F-actin even after SDS treatment (Figures 4 and 5). To further delimit the ^{125}I-F-actin binding site within this 139−295 region, an epitope library expressing protein epitopes of 16−50 amino acids encoded by the inserted 50−150 bp DNA fragments was made, as shown in Figure 6A. A total of 4000 TvecCB/tet colonies from this library were screened for ^{125}I-F-actin binding on bacterial

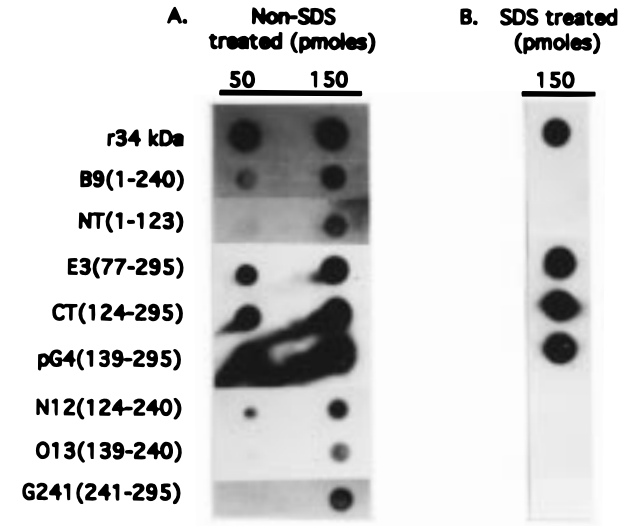

FIGURE 5: Weak interactions with ^{125}I-F-actin on blots exposed under non-SDS denaturing conditions. Autoradiograms of ^{125}I-F-actin overlays of nitrocellulose membranes dot-blotted with native and non-SDS-denatured proteins (50 and 150 pmol) (A) and previously SDS-denatured proteins (150 pmol) (B).

colony blot overlays, but no positive clone was obtained. Another 12 000 colonies from 3 other independently generated 50−150 bp DNA fragment libraries were also analyzed for F-actin binding, but with no success. Consequently, a library expressing larger epitopes of 50−100 amino acids from the inserted 150−300 bp DNA fragments was constructed. The 150−300 bp DNA insert library yielded 33 positive primary clones out of 4000 colonies. In the subsequent secondary screen, 30 out of the initial 33 clones remained positive. Bacterial colony PCR was performed to determine the sizes of the DNA inserts in these 30 clones (data not shown). The average size of the DNA fragments in the positive TvecCB/tet clones was 250 bp, and DNA fragments of ≤250 bp were sequenced. In addition, the DNA inserts of several clones expressing in-frame fragments of 34 kDa protein that did not bind F-actin were also sequenced. The smallest linear region within the 139−295 that conferred ^{125}I-F-actin binding was amino acid residues 193−254 (Figure 6B). The four amino acid residues 193−196 (VNKR) are presumed to contribute to F-actin binding, since the expressed region of 197−295 did not bind the iodinated actin probe. Moreover, the region 241−254 is also required for actin binding as all recombinant truncated proteins terminating at amino acid residue 240 did not bind ^{125}I-F-actin following denaturation by SDS (Figures 4 and 5). The 197−236 portion of this linear ^{125}I-F-actin binding site may also contribute to actin binding as the expressed segment of 237−273 did not bind actin (Figure 6B).

Cosedimentation with F-Actin in Solution. The ability of the truncated forms of the 34 kDa protein to interact with F-actin in solution was studied by the high-speed F-actin cosedimentation assay. In the absence of F-actin, the purified proteins did not sediment under high centrifugal forces and remained in the supernatant (data not shown). However, in the presence of F-actin, only the E3 (77−295), CT (124−295), pG4 (139−295), and r34 kDa proteins were found with F-actin in the pellet (Figure 7). The common region among these four F-actin cosedimenting proteins is the sequence 139−295, as was observed in the SDS-denatured ^{125}I-F-actin binding blot overlay assays (Figures 4 and 5). The B9 (1−

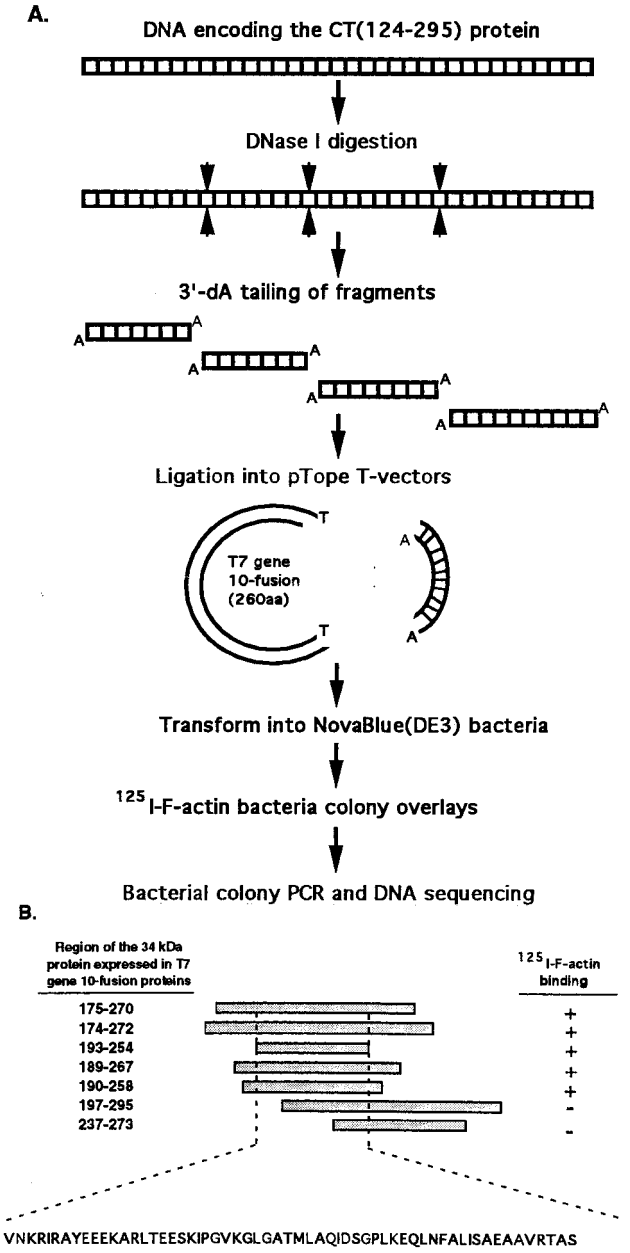

FIGURE 6: Mapping of the ^{125}I-F-actin binding site. (A) Schematic diagram of the NovaTope epitope mapping system to identify the ^{125}I-F-actin binding site in the 34 kDa protein. A library of TvecCB/tet bacteria expressing small peptide segments of the 34 kDa protein as T7 gene 10-fusion proteins was generated by random DNase I digestion of the encoding DNA, ligation of the sized DNA fragments into the T-vector, and transformation of the host bacteria. The library was screened by bacterial colony ^{125}I-F-actin blot overlays. (B) The 34 kDa protein segments that were expressed in-frame with the T7 gene 10-fusion, their ^{125}I-F-actin binding activities, and the sequence of the smallest region in the 34 kDa protein that bound ^{125}I-F-actin on blots.

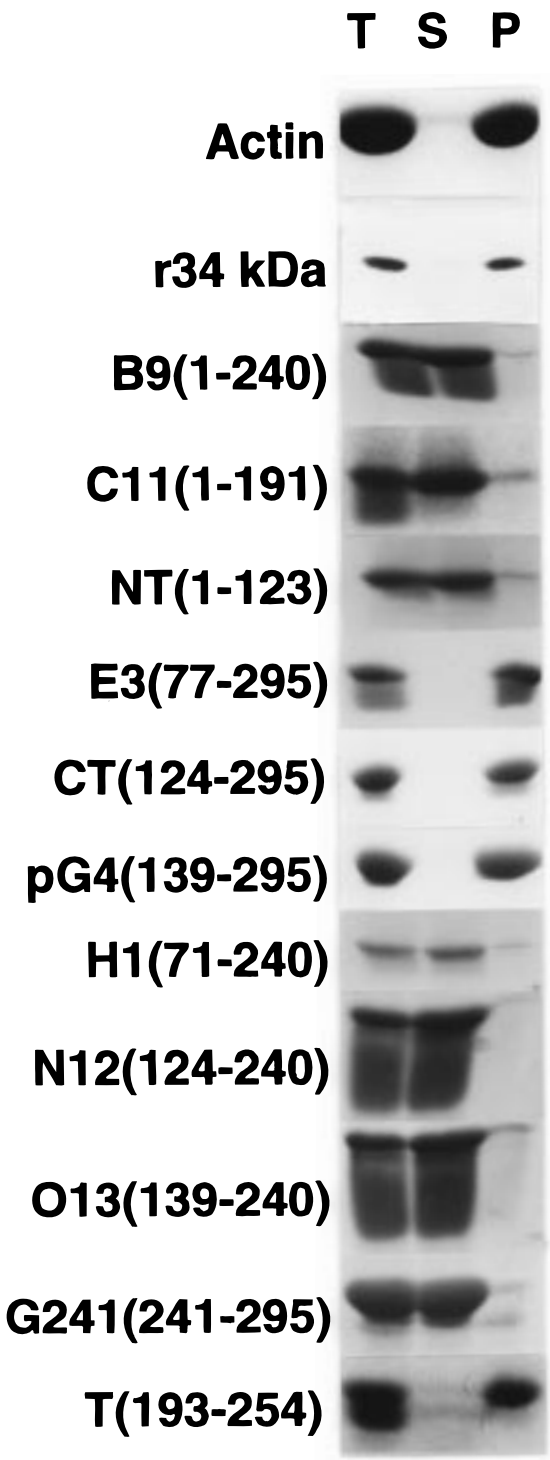

FIGURE 7: Binding of the full-length and truncated 34 kDa proteins to F-actin in solution. Coomassie Blue stained 15% SDS−PAGE gels of the total mixture prior to centrifugation (T), supernatant (S), and pellet (P) samples of F-actin cosedimentation assays. Full-length 34 kDa protein and the various truncated 34 kDa proteins (2.2−10 μM) were mixed with actin (22 μM), and separated into the supernatant and the pellet fractions by high-speed centrifugation. Proteins that bound strongly to F-actin in solution were found with the F-actin in the pellet.

240), C11 (1−191), NT (1−123), H1 (71−240), N12 (124−240), O13 (139−240), and G241 (241−295) proteins did not cosediment with F-actin (Figure 7) although they had exhibited weak ^{125}I-F-actin binding on blots (Figure 5A). Attempts to determine the interactions of the purified T7 gene 10-fusion proteins with F-actin were aborted as the purified T7 gene 10-fusion proteins were prone to aggregation and did not remain soluble even in the presence of detergents and reducing agents. The 62 amino acid region (193−254) identified as a TvecCB/tet clone could not be used directly for cosedimentation assays due to the insolubility of the T7 gene 10 leader. This 62 amino acid region was cloned, expressed, and purified as a thioredoxin fusion protein, T193 (193−254). T193 (193−254) was also able to cosediment with F-actin (Figure 7), while the thioredoxin leader alone did not (data not shown).

Falling-Ball Viscometry. When actin filaments in solution are cross-linked into a meshlike gel by actin binding proteins, the apparent viscosity of the solution increases. Further cross-linking and rearrangement to form bundles result in a decrease in viscosity (*36*). Cross-linking by a monomeric protein would require at least two actin binding sites. Both the monomeric 34 kDa protein and the 27 kDa fragment have been shown to interact with F-actin and to increase the viscosity of the F-actin solution (*15*, *16*, *18*). This assay was conducted to determine whether any of the truncated proteins was capable of altering the viscosity of an F-actin solution in a similar manner as the 34 kDa protein and the 27 kDa fragment by cross-linking actin filaments. Only the E3 (77−295), CT (124−295), and pG4 (139−295) proteins increased the apparent viscosity of the F-actin (4.7 μM) solution (data not shown). The concentration of these three proteins at which the viscosity increased sharply (gel point), $\leq$0.1 μM, was comparable to that demonstrated for the native 34 kDa and r34 kDa proteins (*10*, *18*) and the 27 kDa fragment (*16*). Again, the common region of 139−295 was observed among the truncated proteins that could increase the viscosity of the F-actin solution. Moreover, a preparation of the pG4 (139−295) protein that was monomeric and used directly from a gel filtration column was able to cross-link actin filaments (data not shown). This suggested that there may be two actin binding sites within this 139−295 region of the 34 kDa protein.

Inhibition of F-Actin Disassembly. Some truncated forms of the 34 kDa protein exhibited weak actin binding activity in ^{125}I-F-actin overlay assays that were detected only in the absence of denaturation (Figure 5A). Their association with F-actin might lack sufficient stability to enable cosedimentation with F-actin during high-speed centrifugation (Figure 7). Hence, an actin binding assay that does not require the physical separation of bound and free proteins was employed to reveal any subtle interactions with actin filaments. The native *D. discoideum* 34 kDa protein inhibited the rate of F-actin disassembly under depolymerization conditions by binding to the side and not to either end of pyrene-labeled actin filaments (*14*). A concentration of 2 μM of pyrene-labeled actin was polymerized overnight, and diluted 20-fold under polymerization conditions to the critical actin concentration of 0.1 μM to initiate F-actin disassembly. The rate of disassembly was measured in the absence (control) and presence of the α-chymotryptic digest 27 kDa fragment, the 2 kDa synthetic peptide 279−295, or the NT (1−123) protein. The F-actin disassembly rates were normalized to the control rate (Figure 8). The F-actin disassembly rates were significantly retarded, with the largest 27 kDa fragment having the greatest effect and the smallest 2 kDa synthetic peptide 279−295 having the least inhibition. The estimated K_{app} values of the 27 kDa fragment, the NT (1−123) protein, and the peptide 279−295 are 14 nM, 0.11 μM, and 2.7 μM, respectively.

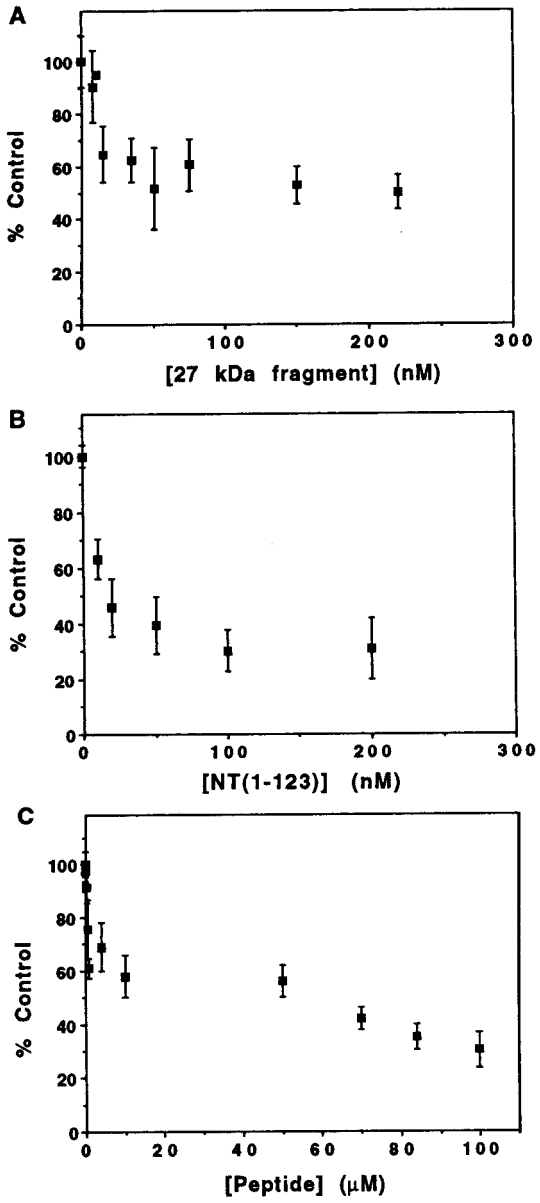

FIGURE 8: Inhibition of the disassembly of pyrene-labeled F-actin by fragments of the 34 kDa protein. The rates of depolymerization of pyrene-labeled F-actin (2 μM diluted to 0.1 μM) were monitored in the absence (control) and in the presence of increasing concentrations of the α-chymotryptic digest 27 kDa fragment (A), the NT (1−123) protein (B), or the 2 kDa synthetic peptide 279−295 (C). The F-actin disassembly rates obtained in the presence of the truncated 34 kDa proteins were normalized to that of the control F-actin disassembly rates. Each data point is mean ± SE, $n = 8$.

DISCUSSION

Members of the actin cross-linking superfamily can be subdivided into several subfamilies based on the homology of their actin binding sites and the modular organization of their functional domains (*37*−*39*). Extensive sequence alignments of the 34 kDa protein with other actin binding proteins revealed no conserved amino acid residues that might be involved in binding actin filaments. The sole cDNA sequence that has homology to the 34 kDa protein cDNA is that of a developmentally regulated gene found in the acellular slime mold *Physarum polycephalum.* The encoded protein of 279 amino acid residues has a 76% identity and 85% similarity to the 34 kDa protein (*40*). The homology is too high for any meaningful prediction of specific conserved regions as actin binding sites in both of these proteins. Alternative approaches to identify the actin binding sites in the 34 kDa protein were sought using direct biochemical analyses of expressed recombinant truncated forms of the 34 kDa protein.

The ^{125}I-F-actin blot overlay assay, the low-shear falling-ball viscometry assay, and the pyrene-labeled F-actin disassembly assays were employed to expose potentially more subtle actin binding activities that would not have been revealed by the commonly used F-actin cosedimentation assay.

Number of Actin Binding Sites Determined by Cosedimentation. The binding of the 34 kDa protein to F-actin exhibits positive cooperativity, and is affected by the length of the actin filaments. Hill coefficients of 1.9 and 3 were obtained for solutions containing actin filament lengths of 4.9 and 0.6 μm, respectively. Thus, at least three actin binding sites contribute to interaction of the 34 kDa protein with actin. Previous results showed that the degree of ordering within bundles containing the 34 kDa protein and F-actin was length-dependent (*34*). Bundles containing short filaments were more ordered than those containing long filaments at the filament lengths and actin concentration (24 μM) used for the binding studies. The difference in the Hill coefficient observed using long versus short filaments likely reflects the nature of the cross-linked structures formed. Two actin binding sites would be sufficient to cross-link the long filaments into a less ordered structure. Formation of highly ordered bundles with shorter filaments involves greater cooperativity of binding, perhaps resulting from contributions of a third actin binding site to intermolecular binding to orient the filament into the bundle geometry. It is important to note that while the 34 kDa protein is monomeric in solution (*15*), formation of a dimeric form in the presence of F-actin remains a formal possibility. Thus, the three actin binding sites reflected in the Hill coefficient could reside within a monomer, or could reflect interactions among two or more 34 kDa protein molecules to form a cross-link. The present data do not allow us to distinguish among these possibilities.

Actin Binding Site Mapped by ^{125}I-F-Actin. The smallest region of the 34 kDa protein that bound ^{125}I-labeled F-actin on blots was localized to a stretch of 62 amino acid residues, 193−254 (Figures 3−6). The intact sequence 193−254 appears to be required for strong F-actin binding and was also able to cosediment with F-actin (Figure 7). Recombinant truncated proteins containing part of the 62 residue sequence were unable to bind F-actin in the high-speed cosedimentation assay (Figure 7) nor bind ^{125}I-F-actin under denaturing conditions (Figures 4−6). The T7 gene 10-fusion proteins of 197−295 and 237−273 from the NovaTope library did not bind ^{125}I-F-actin on blots after denaturation with 6 M urea (Figure 6), and none of the truncated 34 kDa proteins that terminated at or began after amino acid residue 240 (124−240; 139−240; and 241−295) bound ^{125}I-F-actin after treatment with SDS (Figures 4 and 5), although weak binding was observed with high amounts of non-SDS denatured proteins (Figure 5). This suggests that some protein conformation might be involved in ^{125}I-F-actin binding and/or that certain protein structures may be more resistant to SDS denaturation. Additional knowledge regarding the amino acids most important for the interaction with F-actin cannot be obtained by simple truncations at either end of this 62 residue sequence.

Using the Chou and Fasman algorithms (*41*, *42*), this 62 residue sequence is predicted to have α-helices at both the start (193−211) and the end (235−254). It is interesting to note that the first helical region, VNKRIRAYEEEKARLTEES, contains the highly charged consensus sequence RAKA-EEEK-KAAEE previously described to have sequence similarities with cytovillin/ezrin (*43*, *44*) and the repeat sequences in chicken gizzard caldesmon (*17*). These repeat sequences are located within the spacer region of amino acid residues (250−400) of the chicken gizzard caldesmon and are not known to contribute to the actin binding activities of caldesmon (*45*). The helices of the 62 residue sequence are predicted to have more charged residues concentrated on one side than on the opposite side of the helices. It is possible that these two α-helical regions form a V-shaped bipartite actin binding site not unlike that described for the calponin homology domains identified within the actin binding site of α-actinin (*45*, *46*), and which are the fundamental structural elements of the family of proteins that share this actin binding domain (*47*). However, there is little sequence homology between the 62 residue sequence and the calponin homology domain. Moreover, this 62 residue sequence does not have any homology with the C-terminal 34 residue actin binding site identified by ^{125}I-F-actin blot overlays of membrane proteins, moesin, ezrin, and radixin (*48*). This 62 residue sequence also lacks significant homology with drebrin and ponticulin, which bind ^{125}I-F-actin in blot overlays (*35*). Thus, conformational similarity and/or ease of renaturation rather than sequence homology can most easily account for F-actin binding. In accordance with the bipartite actin binding site hypothesis, recombinant proteins containing part of the 62 residue sequence would have possessed only one of the two predicted helical regions. Future crystal structure and NMR studies of the full-length 34 kDa protein and the 62 residue peptide will shed light on the structure and function of this actin binding site.

C-Terminal Actin Binding Site. The truncated proteins E3 (77−295), CT (124−295), and pG4 (139−295) were able to increase the apparent viscosity of F-actin solutions significantly at concentrations less than or equal to that of the 34 kDa protein (Figure 2) (*16*). Thus, these proteins efficiently cross-linked actin filaments, consistent with the presence of two actin binding sites within the shared region of 139−295. One site is the 62 residue sequence 193−254 identified by ^{125}I-F-actin bacterial colony overlays of the NovaTope library, and a second site could be located within the region 255−295. The extreme C-terminus of the 34 kDa protein is highly charged with basic amino acid residues lysine and arginine. Synthetic poly-lysine has been shown to bundle actin filaments (*36*, *49*). Lysine-rich sequences from naturally occurring proteins have been demonstrated to interact with the more acidic actin, and are found in consensus actin binding sites of troponin I, cofilin, myosin, EF-1α (*50*), the villin C-terminal headpiece domain (*51*, *52*), and the myristoylated alanine-rich C-kinase substrate, MARCKS (*53*). A 2 kDa synthetic peptide (norleucine-NRDLEEKKKRYGPQKKK) corresponding to the C-terminal last 17 amino acid residues of the 34 kDa protein was analyzed for actin binding activity. The truncated protein, G241 (241−295), containing these 17 amino acid residues bound F-actin weakly in the absence of SDS on blot overlays (Figure 5A), but did not bind F-actin in the cosedimentation assay (Figure 7). Thus, the F-actin disassembly assay was used to confirm the presence of an additional actin binding site in this region. The ability of the synthetic peptide to

inhibit actin filament depolymerization at the critical concentration (Figure 8) is evidence of direct interaction of the peptide with actin filaments. The affinity (K_{app} 2.7 μM) indicates that the binding is much weaker than that of both the full-length protein (K_{app} 4 nM) (*14*) and the 27 kDa fragment (K_{app} 14 nM). Consistent with the low affinity of the COOH-terminal peptide in the disassembly assay, the G241 (241−295) protein failed to cosediment with F-actin during high-speed centrifugation. The 27 kDa fragment, which is missing the extreme C-terminal ~7 kDa region, could cross-link and cosediment with F-actin but was unable to bundle F-actin (*16*). These results suggest that the COOH-terminal region is important for formation of highly oriented cross-linked bundles by the 34 kDa protein.

NT (1−123) Actin Binding Site. The α-chymotryptic digest 27 kDa fragment is monomeric and possesses F-actin cross-linking activity, consistent with the presence of two F-actin interacting regions within this molecule (*16*). The 27 kDa fragment contains the 62 residue actin binding site (193−254), but lacks the extreme C-terminal F-actin binding site (279−295) of the 34 kDa protein. A third actin binding region of the 34 kDa protein was localized to the N-terminal (1−123) by the non-SDS-denatured ^{125}I-F-actin dot blot overlay assay (Figure 5A) and by the inhibition of F-actin disassembly (Figure 8). Binding of ^{125}I-F-actin on a dot blot was observed at 150 pmol of NT (1−123) protein, but was not detected at the lower amount of 50 pmol (Figure 5A). In addition, the binding was lost upon SDS treatment (Figure 5B), suggesting that this interaction was dependent on protein conformation. The data from the F-actin disassembly assay provided direct evidence that the NT (1−123) protein does indeed interact with filaments with a K_{app} of 0.11 μM (Figure 8), although it fails to cosediment with F-actin during high-speed centrifugation (Figure 7). This suggested that the binding activity of NT (1−123) was weak as compared to the full-length protein and the 27 kDa fragment, and comparison of the values of K_{app} in the disassembly assay is consistent with this interpretation.

Three distinct regions capable of interacting with actin filaments have been localized in the sequence of the 34 kDa protein. The positive cooperative binding of the intact 34 kDa protein to F-actin is an independent measurement indicating interaction among at least three actin binding sites. There appears to be one strong actin binding site (193−254) and two weaker binding sites as assessed using the cosedimentation and disassembly assays. The dependence of the Hill coefficient on the filament length supports the hypothesis that one of the binding sites aids in aligning the filaments in a parallel fashion which was suggested previously from distinct experimental approaches (*16*). However, since the three actin binding sites were dissected and examined separately from the rest of the molecule, it is difficult to discern the contributions of each site to the collective function of the whole molecule. Future studies of the 34 kDa molecule altered to compromise the activity of the first, second, or third actin binding site may shed additional light on the roles of the three sites in F-actin cross-linking and bundling. A complete characterization will also require knowledge of the folding of the 34 kDa protein, the conformational changes that occur upon calcium binding, and the region(s) on the actin filament with which each of the three actin binding sites interacts.

REFERENCES

1. Schleicher, M., and Noegel, A. A. (1992) *New Biol. 4*, 461−472.
2. Condeelis, J. (1993) *Annu. Rev. Cell Biol. 9*, 411−444.
3. Noegel, A. A., and Luna, E. J. (1995) *Experientia 51*, 1135−1143.
4. Rivero, F., Furukawa, R., Noegel, A. A., and Fechheimer, M. (1996) *J. Cell Biol. 135*, 965−980.
5. Rivero, F., Köppel, B., Peracino, B., Bozzaro, S., Siegert, F., Weijer, C. J., Schleicher, M., Albrecht, R., and Noegel, A. A. (1996) *J. Cell Sci. 109*, 2679−2691.
6. Cox, D., Wessels, D., Soll, D. R., Hartwig, J., and Condeelis, J. (1996) *Mol. Biol. Cell 7*, 803−823.
7. de Hostos, E. L., Rehfueb, C., Bradtke, B., Waddell, D. R., Albrecht, R., Murphy, J., and Gerisch, G. (1993) *J. Cell Biol. 120*, 163−173.
8. Faix, J., Steinmetz, M., Boves, H., Kammerer, R. A., Lottspeich, F., Mintert, U., Murphy, J., Stock, A., Aebi, U., and Gerisch, G. (1996) *Cell 86*, 631−642.
9. Furukawa, R., and Fechheimer, M. (1997) *Int. Rev. Cytol. 175*, 29−90.
10. Fechheimer, M. (1987) *J. Cell Biol. 104*, 1539−1551.
11. Furukawa, R., Butz, S., Fleischmann, E., and Fechheimer, M. (1992) *Protoplasma 169*, 18−27.
12. Furukawa, R., and Fechheimer, M. (1994) *Cell Motil. Cytoskel. 29*, 46−56.
13. Fechheimer, M., Ingalls, H. M., Furukawa, R., and Luna, E. J. (1994) *J. Cell Sci. 107*, 2393−2401.
14. Zigmond, S. H., Furukawa, R., and Fechheimer, M. (1992) *J. Cell Biol. 119*, 559−567.
15. Fechheimer, M., and Taylor, D. L. (1984) *J. Biol. Chem. 259*, 4514−4520.
16. Fechheimer, M., and Furukawa, R. (1993) *J. Cell Biol. 120*, 1169−1176.
17. Fechheimer, M., Murdock, D., Carney, M., and Glover, C. V. C. (1991) *J. Biol. Chem. 266*, 2883−2889.
18. Lim, R. W. L., and Fechheimer, M. (1997) *Protein Expression Purif. 9*, 182−190.
19. Sambrook, J., Fritsch, E. F., and Maniatis, T. (1989) *Molecular Cloning, A Laboratory Manual*, 2nd ed., Cold Spring Harbor Laboratory Press, Cold Spring Harbor, NY.
20. Sanger, F., Nicklen, S., and Coulson, A. R. (1977) *Proc. Natl. Acad. Sci. U.S.A. 74*, 5463−5467.
21. Spudich, J. A., and Watt, S. (1971) *J. Biol. Chem. 246*, 4866−4871.
22. MacLean-Fletcher, S. D., and Pollard, T. D. (1980) *Biochem. Biophys. Res. Commun. 96*, 18−27.
23. Schwartz, M. A., and Luna, E. J. (1986) *J. Cell Biol. 102*, 2067−2075.
24. Wuestehube, L. J., and Luna, E. J. (1987) *J. Cell Biol. 105*, 1741−1751.
25. Chia, C. P., Hitt, A. L., and Luna, E. J. (1991) *Cell Motil. Cytoskel. 18*, 164−179.
26. Cooper, J. A., Bryan, J., Schwab, B., Frieden, C., and Loftus, D. J. (1987) *J. Cell Biol. 104*, 491−501.
27. Furukawa, R., Kundra, R., and Fechheimer, M. (1993) *Biochemistry 32*, 12346−12352.
28. Fechheimer, M., and Furukawa, R. (1991) *Methods Enzymol. 196*, 84−91.
29. Segel, I. H. (1975) *Enzyme Kinetics*, John Wiley and Sons, Inc., New York.
30. MacLean-Fletcher, S. D., and Pollard, T. D. (1980) *J. Cell Biol. 85*, 414−428.
31. Smith, P. K., Krohn, R. I., Hermanson, G. T., Mallia, A. K., Gartner, F. H., Provenzano, M. D., Fujimoto, E. K., Goeke, N. M., Olson, B. J., and Klenk, D. C. (1985) *Anal. Biochem. 150*, 76−85.
32. Laemmli, U. K. (1970) *Nature (London) 227*, 680−685.
33. Towbin, H., Staehelin, T., and Gordon, J. (1979) *Proc. Natl. Acad. Sci. U.S.A. 76*, 4350−4354.
34. Furukawa, R., and Fechheimer, M. (1996) *Biochemistry 35*, 7224−7232.
35. Luna, E. J., Pestonjamasp, K. N., Cheney, R. E., Strassel, C. P., Lu, T. H., Chia, C. P., Hitt, A. L., Fechheimer, M.,

Furthmayr, H., and Mooseker, M. S. (1997) in *Cytoskeletal Regulation of Membrane Function* (Froehner, S. C., and Bennett, V., Eds.) pp 3−18, Rockefeller University Press, New York.
36. Griffith, L. M., and Pollard, T. D. (1982) *J. Biol. Chem. 257*, 9135−9142.
37. Matsudaira, P. (1991) *Trends Biochem. Sci. 16*, 87−92.
38. Hartwig, J. H., and Kwiatkowski, D. J. (1991) *Curr. Opin. Cell Biol. 3*, 87−97.
39. Puius, Y. A., Mahoney, N. M., and Almo, S. C. (1998) *Curr. Opin. Cell Biol. 10*, 23−34.
40. St.-Pierre, B., Couture, C., Larouche, A., and Pallotta, D. (1993) *Biochim. Biophys. Acta 1173*, 107−110.
41. Chou, P. Y., and Fasman, G. D. (1974) *Biochemistry 13*, 222−245.
42. Chou, P. Y., and Fasman, G. D. (1974) *Biochemistry 13*, 211−222.
43. Turunen, O., Winqvist, R., Pakkanen, R., Grzeschik, K.-H., Wahlstrom, T., and Vaheri, A. (1989) *J. Biol. Chem. 264*, 16727−16732.
44. Algrain, M., Turunen, O., Vaheri, A., Louvard, D., and Arpin, M. (1993) *J. Cell Biol. 120*, 129−139.
45. Castresana, J., and Saraste, M. (1995) *FEBS Lett. 374*, 149−151.
46. Carugo, K. D., Banuelos, S., and Saraste, M. (1997) *Nat. Struct. Biol. 4*, 175−179.
47. Goldsmith, S. C., Pokala, N., Shen, W., Fedorov, A. A., Matsudaira, P., and Almo, S. C. (1997) *Nat. Struct. Biol. 4*, 708−712.
48. Pestonjamasp, K., Amieva, M. R., Strassel, C. P., Nauseef, W. M., Furthmayr, H., and Luna, E. J. (1995) *Mol. Biol. Cell 6*, 247−259.
49. Janmey, P. A., Hvidt, S., Lamb, J., and Stossel, T. P. (1990) *Nature 345*, 89−92.
50. Vandekerckhove, J. (1990) *Curr. Opin. Cell Biol. 2*, 41−50.
51. Friederich, E., Vancompernolle, K., Huet, C., Goethals, M., Finidori, J., Vandekerckhove, J., and Louvard, D. (1992) *Cell 70*, 81−92.
52. McKnight, J. C., Matsudaira, P. T., and Kim, P. S. (1997) *Nat. Struct. Biol. 4*, 180−184.
53. Hartwig, J. H., Thelen, M., Rosen, A., Janmey, P. A., Nairn, A. C., and Aderem, A. (1992) *Nature 356*, 618−622.

BI981392D